# Radiating Slot in the Coaxial Cable Shield: Measurement Based Characterization

Antonio Šarolić, Zlatko Živković, Damir Senić, and Niko Ištuk

*Abstract:* **The paper presents the comprehensive experimental study of radiation characteristics of a single slot in a coaxial cable shield. The slot was realized in four different embodiments, which varied by slot orientation and length. Three orthogonal polarizations of radiated electric field were analyzed along the axis perpendicular to cable, broadside to the slot, in a broadband frequency range (80-1000 MHz). The analysis was based on thorough measurements of the coupling loss, which is the common parameter for the leaky cable characterization. The obtained results showed that the electric field component longitudinal to the cable axis considerably dominates over other two orthogonal components, for all four slot types. Doubling the length of the slot caused a ca. 20 dB increase of the radiated field. Different slot orientations, having the same length in the cross-section projection, yielded approximately equal field strengths. The results of this experimental study clearly and visibly demonstrate the radiating slot field dependence on polarization and slot geometry in a wide frequency range. Thus they are useful for planning of wireless communication systems based on radiating cables, as well as for understanding polarization related issues in such systems.**

*Index terms:* **leaky radiating coaxial cable shield, slot length and orientation, coupling loss measurements, polarization**

## I. INTRODUCTION

A slot in an infinite PEC (perfect electric conductor) plane is a well-known theoretically analyzed radiation source [1]. A slot may also be cut in a coaxial cable shield, presenting a radiating element in a leaky or radiating cable system [2-5]. Leaky cables are slotted coaxial structures used as radiation sources for indoor wireless communications (buildings, tunnels, mines, subways, etc. [6-10]), where ordinary antennas present a less suitable solution.

The comprehensive theoretical study of leaky cables [2-5], [11-13], accompanied with numerical and measurement results [14-20], can be found in literature. However, the rigorous analytical approach for a single slot mainly deals with electric field distribution on the slot [2, 4], without a clear insight into the electromagnetic (EM) fields radiated from a single slot. These fields could be of interest, as a single slot can subsequently be treated as an antenna array element on a coaxial cable with a large number of periodically arranged

slots. The radiated fields calculated by using cylindrical harmonic expansion [12], mode matching techniques combined with quasi static [11] or integral [17] methods, as well as numerical procedures [3, 5, 16] require self-developed codes, and their application in practice is not straightforward. On the other hand, a few experimental studies that can be found in literature [6, 7, 15], mainly deal with dominating polarization component that is measured at several cable-to-receiver distances, in a narrow frequency range.

Therefore, this paper presents a measurement-based comprehensive study of the radiation characteristics of a single slot in a coaxial cable shield. The study is based on extensive measurement results for four different slots, having different lengths and orientations, i.e. inclination angles with respect to the cable axis. Coupling loss was measured along the axis perpendicular to cable, broadside to the slot, for three orthogonal electric field polarizations, in a broadband frequency range from 80 MHz to 1000 MHz. The experimental results presented in this paper can be applied by communication engineers while planning leakage cable wireless systems, especially regarding signal coverage issues.

The paper is structured as follows – the second chapter presents the detailed explanation of the materials and methods that were used to characterize radiation properties of a radiating slot, as well as detailed description of the measurement setup. At the end of the chapter the coupling loss calculation, based on the measured quantities, has been presented. The measurement results for the selected slot embodiments and receiving antenna positions were presented and discussed in the third chapter. The concluding remarks are given at the fourth chapter.

## II. MATERIALS AND METHODS

### A. Slot embodiments

Each single slot was positioned in the midpoint of a 1 m long RG213 50 Ω coaxial cable with polyethylene dielectric ($\varepsilon_r$=2.25). The slot was realized in four different embodiments (Table 1), which varied by orientation (90º and 30º to the cable axis), and length (20% and 40% of the cable circumference, measured in the cross-section projection of the slot). Embodiments and relevant dimensions are shown in Fig. 1, where $a$ and $b$ are standard dimensions of the RG213 50 Ω coaxial cable, while the circumference $C$ of the outer conductor is calculated as $C=\pi b$. The slots were made as narrow as possible, to achieve $w \ll l_s$ and $w \ll l_i$.

TABLE I   SLOT EMBODIMENTS

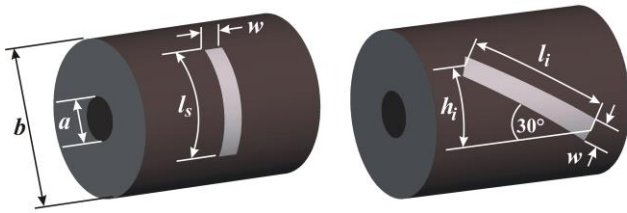| Embodiment | Inclination angle with respect to cable axis | Slot length |
|:---:|:---:|:---:|
| 1 | normal, 90º | $l_s=0.2C$ |
| 2 | normal, 90º | $l_s=0.4C$ |
| 3 | inclined, 30º | $h_i=0.2C$ |
| 4 | inclined, 30º | $h_i=0.4C$ |



Fig. 1. Left: normal slot; Right: inclined slot

## B. Measurement setup

The radiation characteristics of a leaky (radiating) cable, having a large number of slots along a considerable cable length, are commonly measured in accordance with IEC 61196-4 standard [21]. The standard describes coupling loss measurements along the cable axis, at a single predefined radial (broadside direction) distance of 2 m. Relying on the measurement method described in the standard, the intention of this study was to measure the coupling loss along the axis perpendicular to cable, broadside to the slot, varying the distance (i.e. height, according to Fig. 2) from 0.2 m to 2 m with a 10 cm step. Basically, this resulted with the radial coupling loss profiles in front of the slot, measured for three orthogonal polarizations shown in Fig. 2.
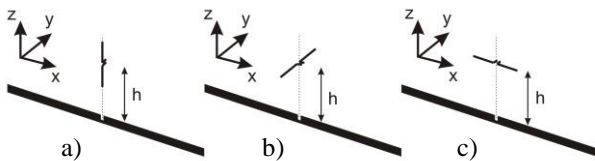


Fig. 2. Three antenna orientations: a) radial; b) transversal; c) longitudinal

The IEC 61196-4 standard [21] suggests two types of measurements methods: the free space method and the ground level method. In the free space method the radiating cable should be positioned on the non-metallic posts at a height of 1.5 to 2 m. The monitoring antenna should be positioned at the same height as that of the examined cable, on the horizontal distance of 2 m from the cable. In the ground level method the cable should be positioned on the non-metallic posts, at a distance of 10-12 cm from the concrete floor. The coupling loss is then measured at the height of 2 m directly above the cable. Considering the available measurement surrounding, the measurements in this study were carried out according to the ground level method.

Even though the given standard recommends the usage of half-wave dipole antenna for measurement purposes, other types of antennas can also be used, provided that their gain is known. For this broadband study, a biconical dipole was used (Fig. 3), as a more convenient broadband antenna. The measured coupling loss was then expressed with respect to the half-wave dipole antenna.

The measurements were performed in the frequency range from 80 MHz to 1 GHz in 1001 discrete frequency points.

The coupling loss was measured using a vector network analyzer Agilent FieldFox N9912A RF Combination Analyzer in CAT (Cable and Antenna Test) mode, measuring the 2-port insertion loss between the output and the input port of the device. Taking into account all the gains and losses in the system, the coupling loss was easily obtained.

The analyzer itself has a nominal output power of +6 dBm, and the preliminary measurements using only that amount of input power showed that the slot generated very weak radiation, i.e. the resulting coupling loss, in addition to the system losses in the connection cables, was rather high compared to the system dynamic range. Therefore, the dynamic range had to be increased by additional gain achieved by a 150W broadband RF amplifier (Amplifier Research AR150W1000). The schematic layout of the measurement setup is shown in Fig. 4a.
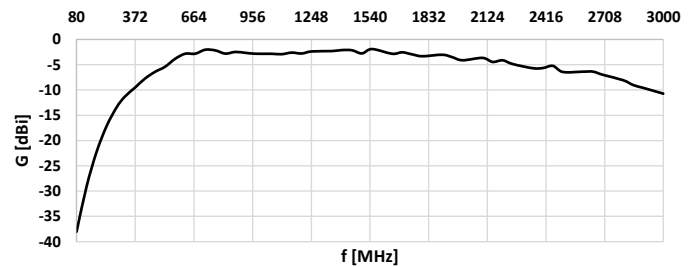


Fig. 3. Gain of the calibrated broadband biconical dipole

The output signal from the analyzer was amplified and fed to the slotted coaxial cable that was terminated by a high power 30 dB attenuator and a 50 Ω dummy load. The electric field radiated by the slot (DUT), was measured by a calibrated broadband biconical dipole antenna PCD 8250 placed directly above the DUT, mounted on the adjustable wooden tripod (Fig. 4b). The RX antenna height was varied from 0.2 m to 2 m with a 10 cm step.

Besides the VNA's own limited dynamic range, the overall measurement system dynamic range was limited by two additional factors. The RX antenna (broadband biconical dipole) gain is shown in Fig. 3, showing a severe deficiency in the lower part of its frequency range, that eventually transforms to the system dynamics limitation. Also, considering the frequency range of interest (from 80 MHz to 1 GHz), the dynamic range was compromised by the background noise and interference arising from various radio systems present in that range. After a comprehensive EM site survey, the measurement location was chosen in the faculty basement where no interference problems had been observed.
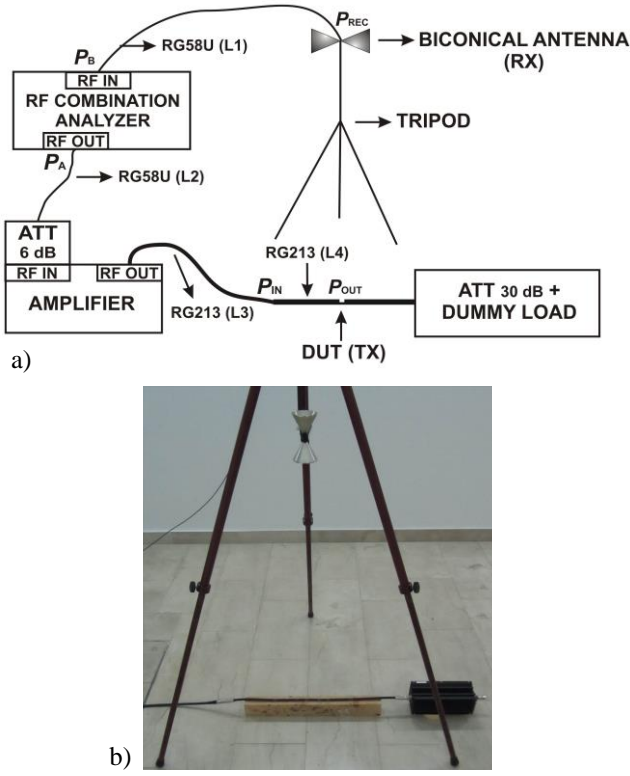
Fig. 4. Measurement setup (DUT denotes the radiating slot)
a) schematic layout, b) biconical dipole antenna above DUT (radial
orientation)

### C. Coupling loss calculation

Coupling loss $CL$ is defined as the difference (in dB) between the power $P_{out}$ in the radiating cable at the location of the slot, and the available power $P_{rec}$ measured at the receiving antenna (Fig.4), placed broadside to the slot, at a certain distance:

$$CL_i\left[dB\right] = P_{out}\left[dBm\right] - P_{rec, i}\left[dBm\right]. \quad (1)$$

Index $i$ stands for $i$-th polarization of the measured electric field. According to Fig. 2, and with respect to the cable axis, polarization can be measured as radial, transversal and longitudinal. According to [21], the receiving antenna is preferably a half-wave dipole, however, other type of antenna can be used, and its type and gain should be given with the results. If the cable attenuation constant $\alpha$ is known, as well as the power $P_{in}$ at the cable input terminal, $P_{out}$ can be calculated as:

$$
\begin{aligned}
P_{out}\left[dBm\right] &= P_{in}\left[dBm\right] - \alpha\left[dB/m\right]\cdot x\left[m\right] = \\
&= P_{in}\left[dBm\right] - L_4\left[dB\right],
\end{aligned} \quad (2)
$$

where $x$ is the distance from the cable input terminal to the slot, and $L_4$ denotes the cable loss calculated using the attenuation constant $\alpha$ previously measured in the frequency range of interest. The distribution of signal powers ($P_{rec}$, $P_A$, $P_B$, $P_{in}$, $P_{out}$) and cable losses ($L_1$, $L_2$, $L_3$, $L_4$), at the points of interest along the system, is also indicated in Fig. 4. Taking into account the attenuation ATT of 6 dB, amplifier gain $G_{amp}$, cables losses $L_2$ and $L_3$, $P_{out}$ can be expressed using $P_A$:

$$
\begin{aligned}
P_{out}\left[dBm\right] &= P_{in}\left[dBm\right] - L_4\left[dB\right] = \\
&= P_A\left[dBm\right] - L_2\left[dB\right] - ATT\left[dB\right] + \\
&+ G_{amp}\left[dB\right] - L_3\left[dB\right] - L_4\left[dB\right].
\end{aligned} \quad (3)
$$

Likewise, $P_{rec}$ can be expressed using $P_B$:

$$P_{rec}\left[dBm\right] = P_B\left[dBm\right] + L_1\left[dB\right] \quad . \quad (4)$$

Hence the coupling loss can be calculated using (1), (3) and (4):

$$
\begin{aligned}
CL\left[dB\right] &= P_A\left[dBm\right] - L_2\left[dB\right] - ATT\left[dB\right] + G_{amp}\left[dB\right] - \\
&- L_3\left[dB\right] - L_4\left[dB\right] - P_B\left[dBm\right] - L_1\left[dB\right]
\end{aligned} \quad (5)
$$

All the losses and gains were known, since they had been previously measured in the frequency range of interest. The difference ($P_A$ - $P_B$) was actually measured by the analyzer as the insertion loss $IL$ (Fig.4):

$$IL\left[dB\right] = P_A\left[dBm\right] - P_B\left[dBm\right]. \quad (6)$$

Thereby, the coupling loss $CL_{bicon}$ (measured by the biconical dipole) was finally deducted as:

$$
\begin{aligned}
CL\left[dB\right] &= IL\left[dB\right] - L_2\left[dB\right] - ATT\left[dB\right] + G_{amp}\left[dB\right] - \\
&- L_3\left[dB\right] - L_4\left[dB\right] - L_1\left[dB\right]
\end{aligned} \quad (7)
$$

The coupling loss obtained by the biconical dipole can be easily converted to the coupling loss with respect to half-wave dipole. Using the Friis equation, $P_{rec}$ can be expressed as a function of the RX antenna gain (all quantities in dB):

$$
\begin{aligned}
CL_{bicon}\left[dB\right] &= P_{out} - P_{rec\_bicon} = \\
&= P_{out} - (P_{out} + G_{slot} + G_{bicon} + 20\log\frac{\lambda}{2\pi r}) \\
&= -G_{slot} - G_{bicon} - 20\log\frac{\lambda}{2\pi r} \quad ,
\end{aligned} \quad (8)
$$

$$
\begin{aligned}
CL_{\lambda/2}\left[dB\right] &= P_{out} - P_{\lambda/2} = \\
&= P_{out} - (P_{out} + G_{slot} + G_{\lambda/2} + 20\log\frac{\lambda}{2\pi r}) \\
&= -G_{slot} - G_{\lambda/2} - 20\log\frac{\lambda}{2\pi r} \quad ,
\end{aligned} \quad (9)
$$

for the biconical and half-wave dipole, respectively. $G_{bicon}$ had been previously measured (shown in Fig.3), and $G_{\lambda/2}$ equals 2.15 dB, the standard gain of the half-wave dipole. After subtracting (8) from (9), $CL_{\lambda/2}$ can be calculated (in dB):

$$CL_{\lambda/2,i}\left[dB\right] = CL_{bicon,i}\left[dB\right] + G_{bicon,i}\left[dB\right] - G_{\lambda/2}\left[dB\right] \quad . \quad (10)$$

Since the coupling loss was measured separately for each of the three orthogonal polarizations (Fig. 2), index $i$ is shown in (10). Therefore, the standard [21] defines the mean coupling loss calculated by:

$$CL_{mean}\left[dB\right] = -10\log\left(\frac{1}{3}\sum_{i=1}^{3}10^{-\frac{CL_i}{10}}\right). \quad (11)$$

## III. RESULTS AND DISCUSSION

### A. Noise level

The measurement dynamics was limited by the instrument noise level. In order to observe this limitation, the noise level was measured in terms of insertion loss, by cutting off the power transmission. This was achieved by turning off the power amplifier, however keeping all the connections, including the RX antenna, to observe eventual background noise and interference received by the antenna.

The measured insertion loss noise, averaged over 30 frequency sweeps, is shown in Fig. 5, showing no background signals, thus approving the choice of measurement location in a quiet environment. The noise level remained practically unchanged for all polarizations. The measured insertion loss noise level was then converted to the coupling loss noise level (also displayed in Fig. 5) using equations (7) and (10), to observe the actual limitation of the measurement system for the quantity of interest. The dynamics starts to drastically decrease below 300 MHz, as a consequence of a very low RX antenna gain (observable in Fig. 3).
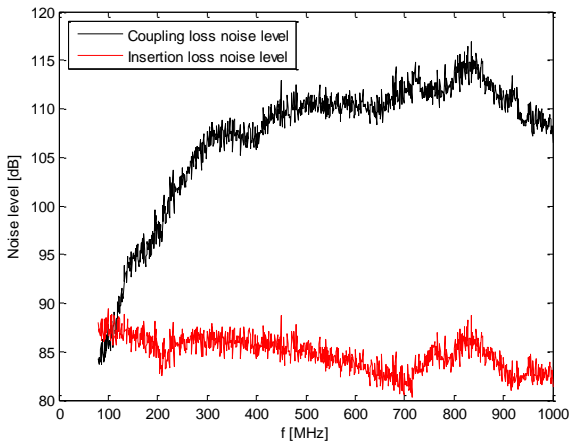


Fig. 5. Insertion loss and coupling loss noise levels

### B. Coupling loss frequency dependence

Fig. 6 and Fig. 7 show the coupling loss in front of the normal slot, for $l_s=0.2C$ and $l_s=0.4C$ respectively, as a function of frequency, at three discrete distances: 20 cm, 1 m and 2 m. The figures show three orthogonal polarizations (according to Fig. 2), along with the noise level. Several observations can be made. The longitudinal polarization considerably dominated over the other two in all cases, by 10 to 20 dB. For the shorter slot and greater distances, the less pronounced polarizations approached the noise level. The coupling loss for the longer slot ($0.4C$) was considerably lower than for the shorter slot ($0.2C$) – most easily observable for the dominant polarization (the lowest curve). Fig. 8 and Fig. 9 show the coupling loss in front of the inclined slot, for $h_i=0.2C$ and $h_i=0.4C$ respectively, as a function of frequency, at three discrete distances: 20 cm, 1 m and 2 m. The figures show three orthogonal polarizations (according to Fig. 2), along with the noise level. It can be observed that the coupling loss was very similar to the normal slot, for the dominant (longitudinal) polarization. Due to the slot inclination, the other two polarizations had a slightly lower coupling loss than with the normal slot. For the mean coupling loss defined by (11), this has no major consequence, since the major part of the mean value is the dominant (longitudinal) polarization, for both slot inclinations. However, this may be important for communication with an antenna polarized orthogonally to the longitudinal polarization, increasing its reception by a few dB.

Generally, at lower heights, the radial component dominated over the transversal component. The certain conclusions about their relation at higher distances cannot be made since their values progressively oscillated with frequency close to the coupling loss noise limit.

Fig. 10 shows only the dominant (longitudinal) polarization, at the height of 2 m (most interesting both for communications and with respect to [21]), for different types of slots. It can be easily noticed that the coupling loss was almost 20 dB lower for the longer slots, $l_s=0.4C$ and $h_i=0.4C$, than for the shorter slots, $l_s=0.2C$ and $h_i=0.2C$. On the other hand, there was no major difference between the slots of the same length, regardless of their inclinations.

Fig. 11 shows only the dominant (longitudinal) polarization, at three different heights of 0.2 m, 1 m and 2 m. The graph is shown for the longer slot only, to achieve better visibility (lower coupling loss). Theoretically, as the distance increases from 0.2 m to 1 m by a factor of 5, the coupling loss should increase by 14 dB. Similar, as the distance increases from 1 m to 2 m by a factor of 2, the coupling loss should increase by 6 dB. The measurement results approximately followed this consideration. The graph is shown only for the normal slot, since Fig. 10 showed that the results for the inclined slot were very similar.

### C. Coupling loss profiles

Fig. 12 shows the coupling loss profiles for the dominant (longitudinal) polarization, at three different frequencies (100 MHz, 500 MHz and 1 GHz) for the normal slot, $l_s=0.4C$. It is observable that the coupling losses at these three frequencies differed by less than 10 dB in any given point. Fig. 13 and Fig. 14 show the coupling loss profiles at three frequencies (100 MHz, 500 MHz and 1 GHz) along the axis perpendicular to the cable, in front of the slot, for the normal and the inclined slot, respectively. Figures refer to the longer slots, $l_s=0.4C$ and $h_i=0.4C$, to achieve better visibility (lower coupling loss). All three polarizations are shown, along with the noise level associated with each frequency. In the radiating far field of the source (slot), a steady increase of the coupling loss is expected as the distance increases. However, graphs show the decrease of the coupling loss for the dominant (longitudinal) polarization at 100 MHz as the distance increases above 120 cm, suggesting that the RX antenna was still in the near field of the source, where such variations commonly occur. This is not strange since the wavelength of 3 m (at 100 MHz) is greater than the distance from the source. At frequencies of 500 MHz and especially at 1 GHz, for the dominant (longitudinal) polarization, there were still some fluctuations of the coupling loss with the distance, probably due to the measurement uncertainty, but the trend is acceptable. It is worth repeating that, theoretically, the coupling loss should increase by 14 dB from 20 cm to 1 m, and by only 6 dB from 1 m to 2 m. This was practically achieved at 500 MHz.
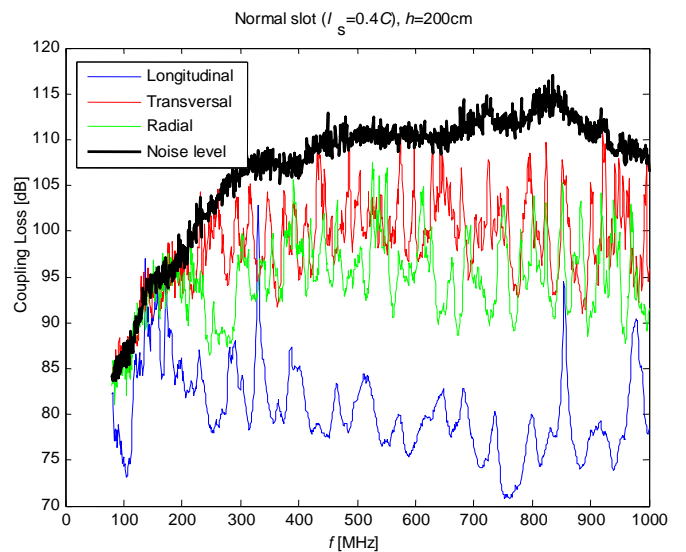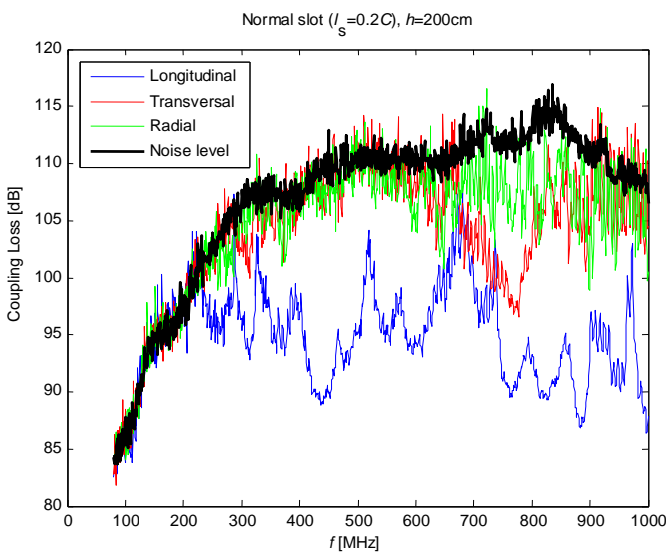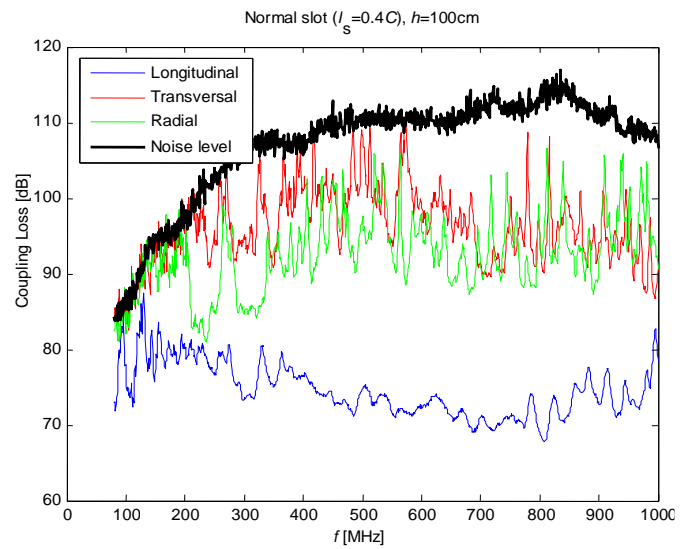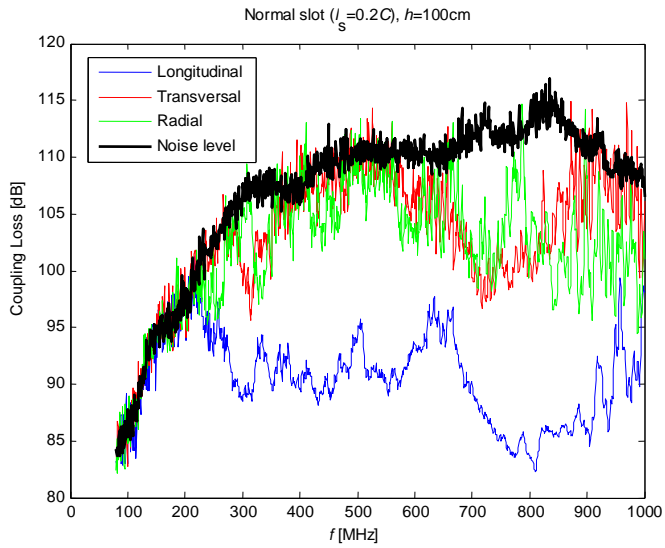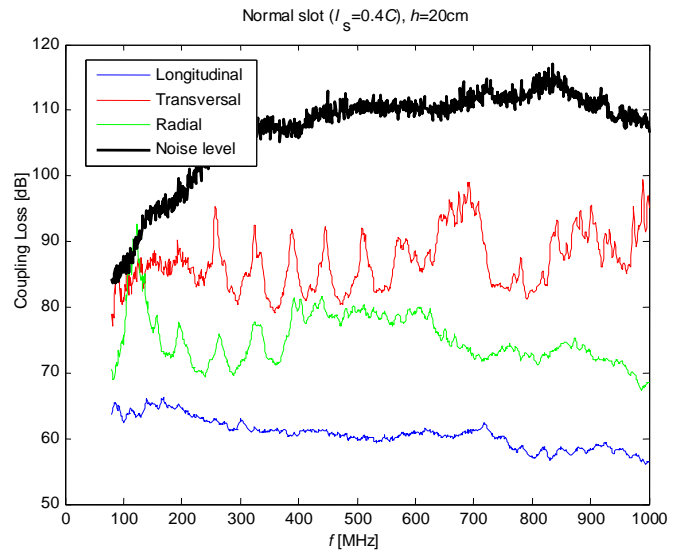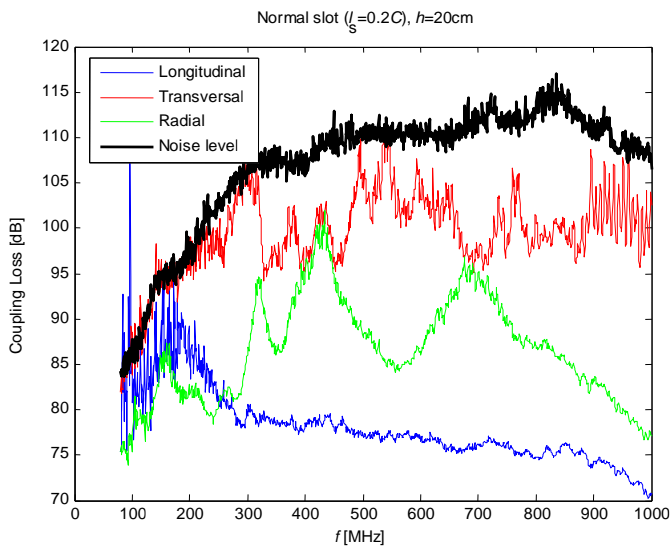
Fig. 6. Coupling loss frequency dependence at specific heights, for normal slot, $l_S$=0.2$C$ (lower coupling loss is better, in all figures)

Fig. 7. Coupling loss frequency dependence at specific heights, for normal slot, $l_S$=0.4$C$
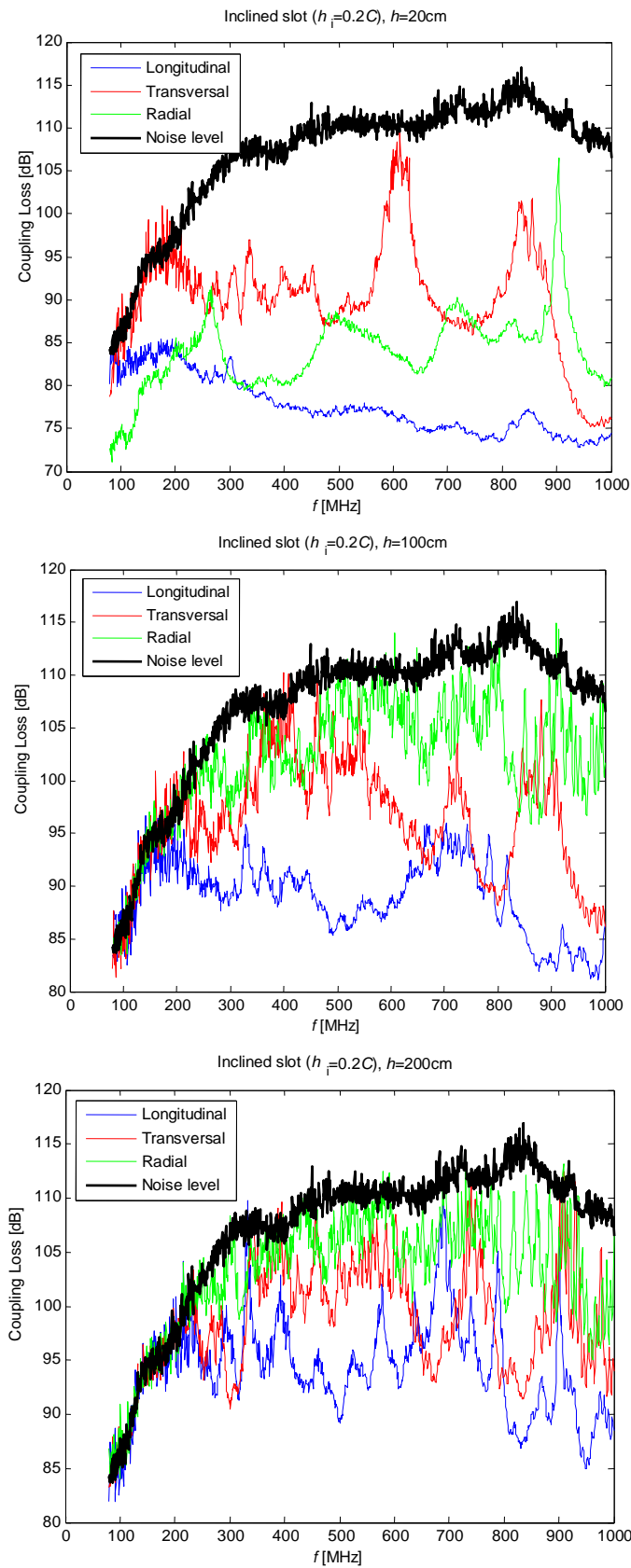
Fig. 8. Coupling loss frequency dependence at specific heights, for inclined slot, $h_i$=0.2$C$
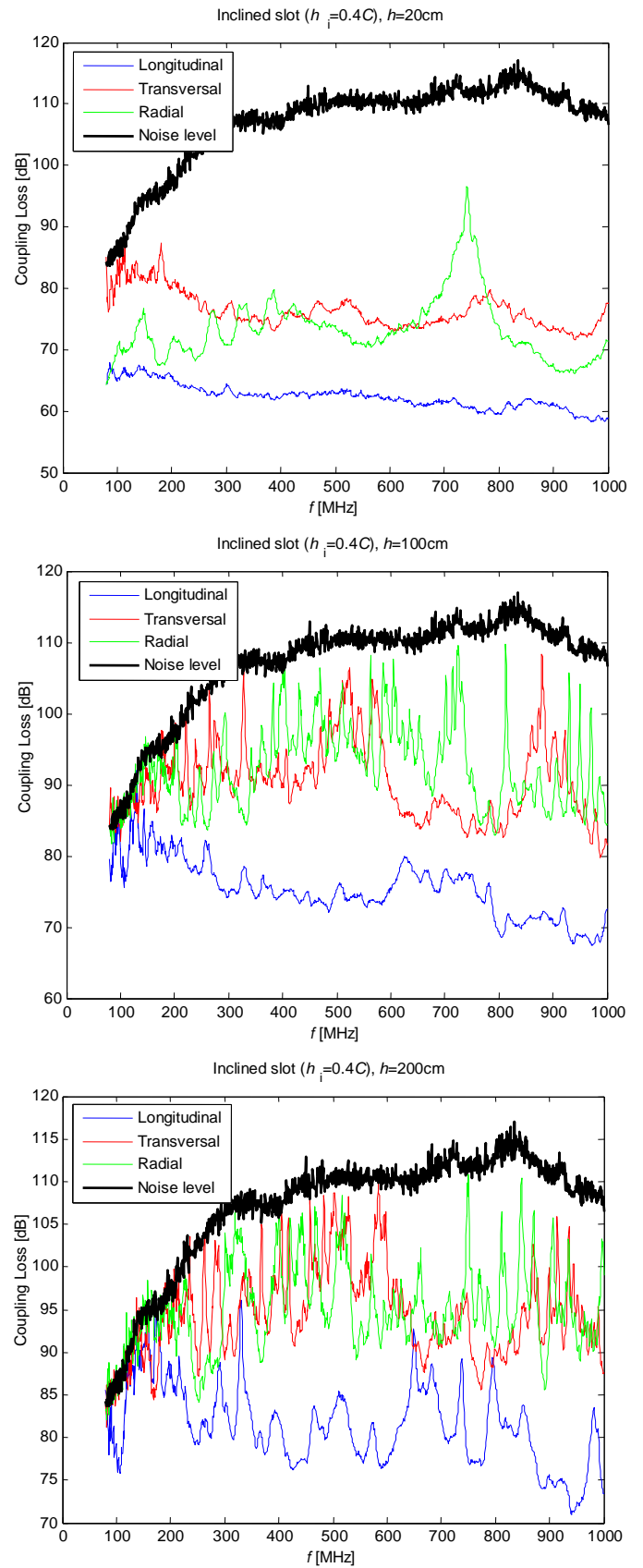
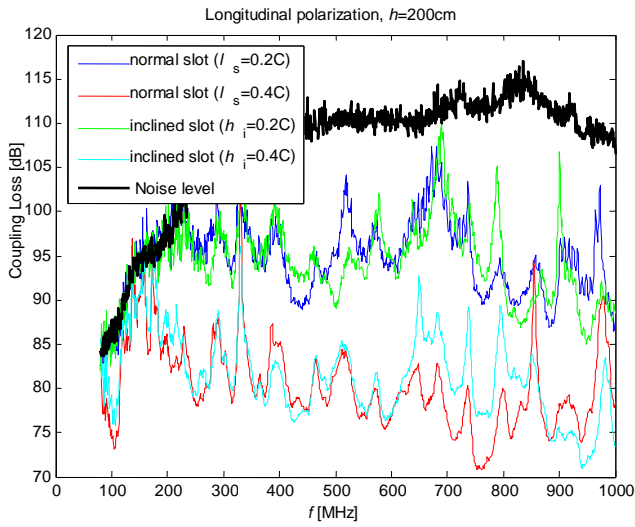Fig. 9. Coupling loss frequency dependence at specific heights, for inclined slot, $h_i$=0.4$C$

Fig. 10. Coupling loss frequency dependence, longitudinal polarization, height $h$=2 m, for different slots
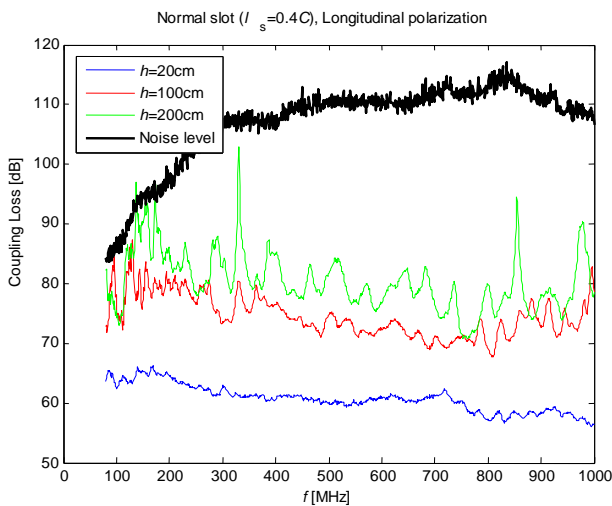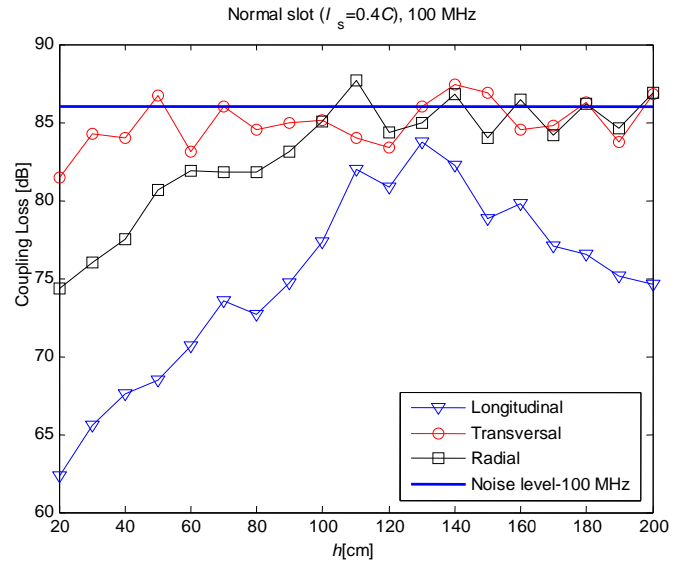


Fig. 11. Coupling loss frequency dependence, longitudinal polarization, normal slot, $l_S$=0.4$C$, for three different heights
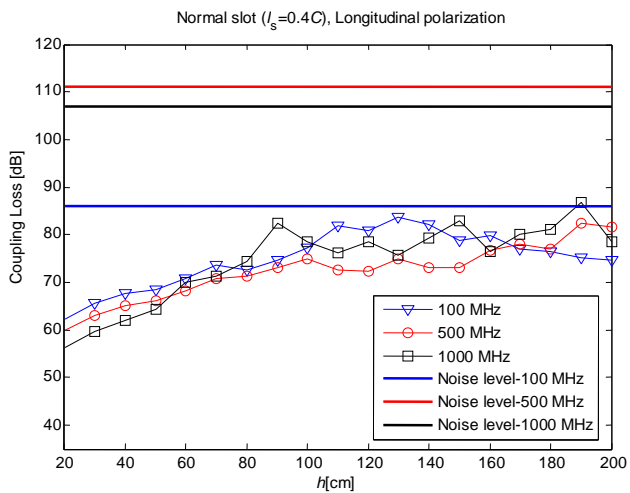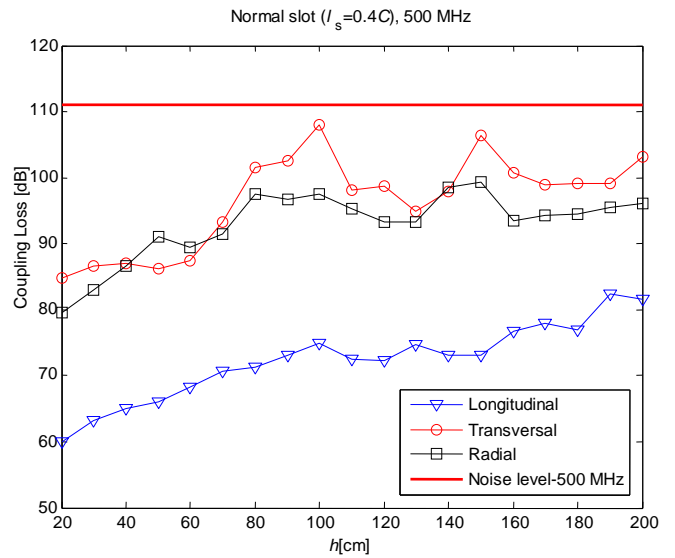


Fig. 12. Coupling loss profiles for the longitudinal polarization, normal slot, $l_S$=0.4$C$, for three different frequencies



Fig. 13. Coupling loss profiles for all three polarizations, normal slot, $l_S$=0.4$C$, for three different frequencies

For the full insight into the measurement results, the 3D graphs of the mean coupling loss, calculated using (11), for all frequencies, heights and slot embodiments, are presented in Fig. 15.
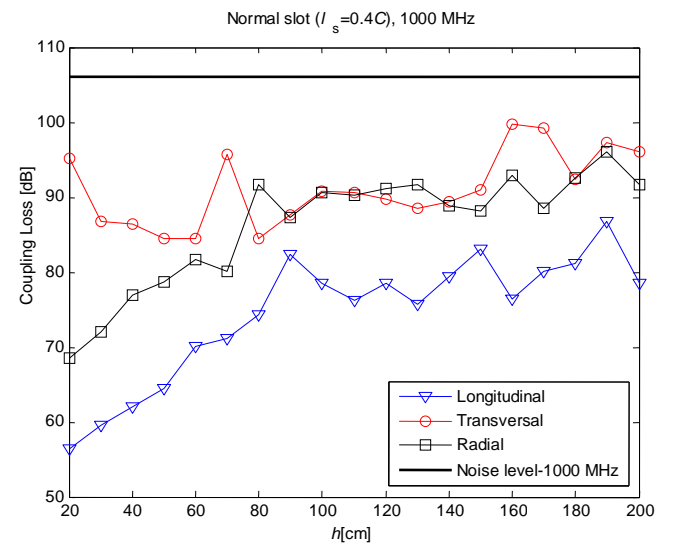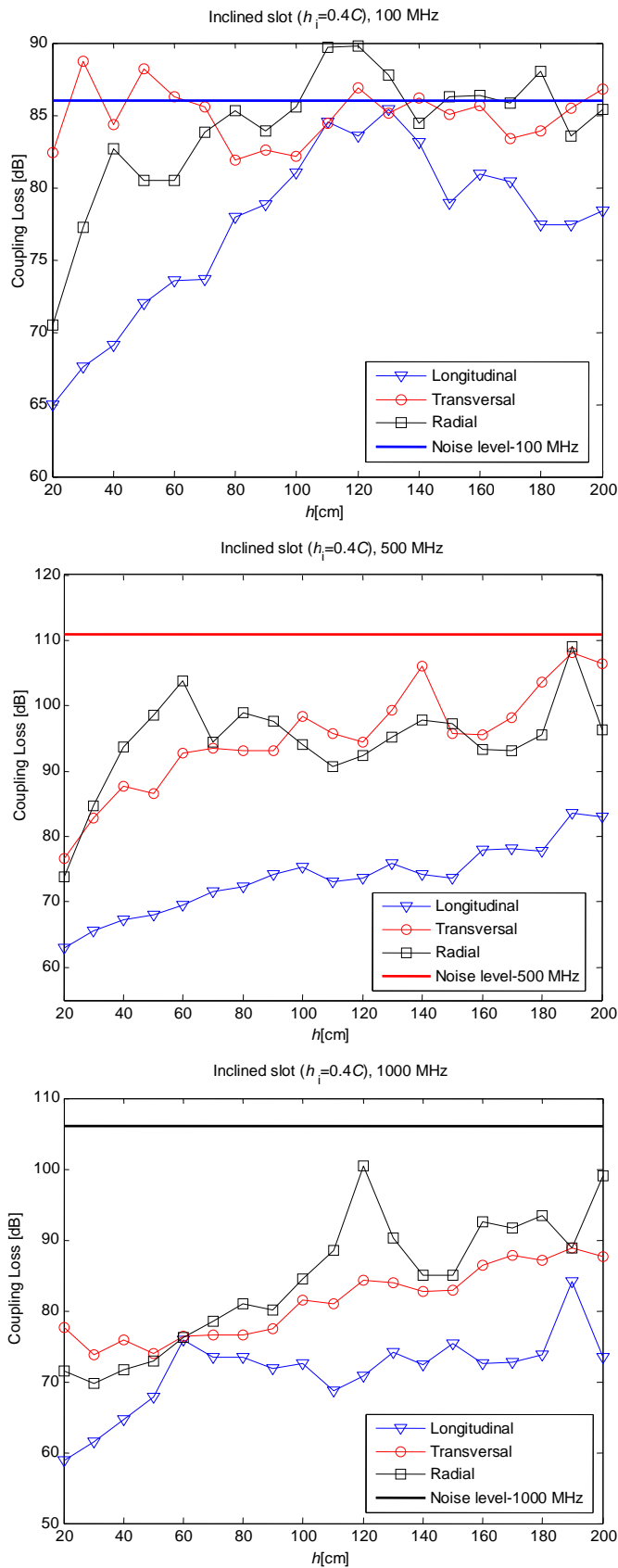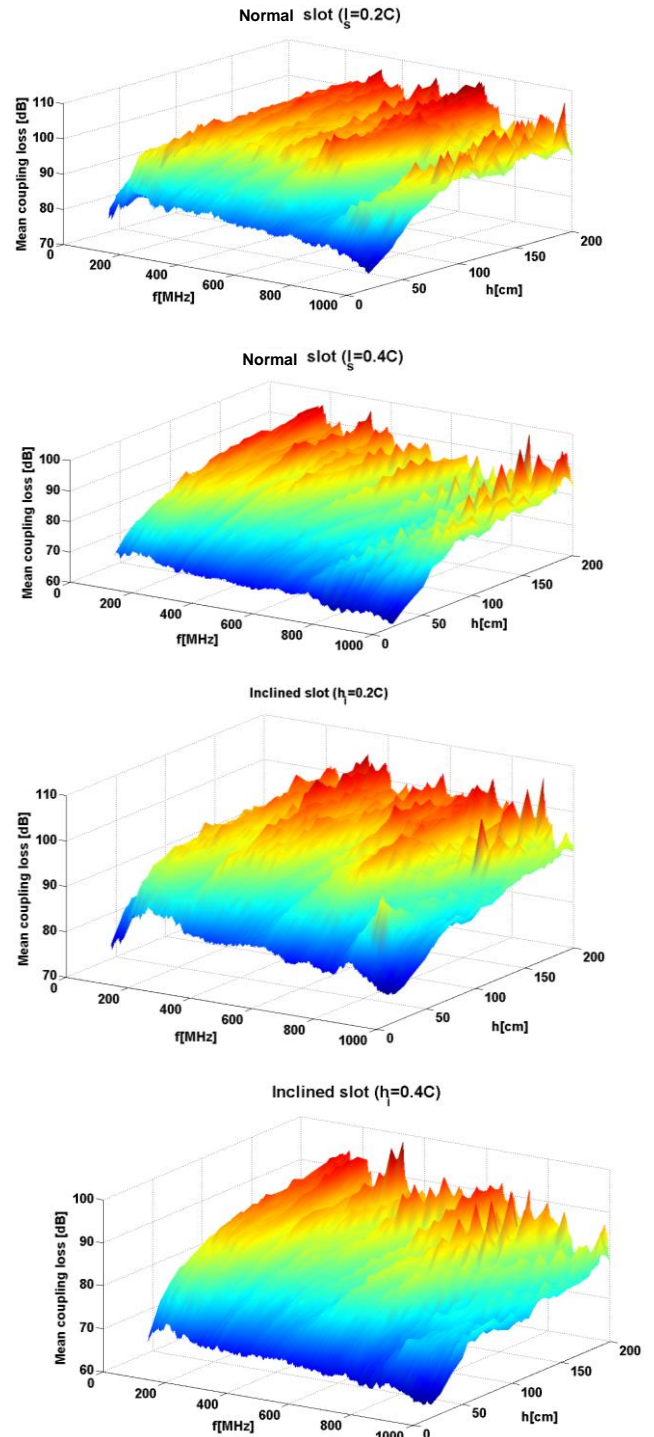


Fig. 14. Coupling loss profiles for all three polarizations, inclined slot, $h_i$=0.4$C$, for three different frequencies



Fig. 15. Mean coupling loss for all slot types

## IV. CONCLUDING REMARKS

A single slot in a coaxial cable shield is a variation of the slot antenna, and can be used both for transmitting EM waves from the cable, and receiving EM waves into the cable. Cables having a large number of periodically arranged slots are commonly used as distributed antennas, so called "leaky cables". Understanding of a single slot radiation is therefore important for the understanding of a leaky cable behavior.

This study consisted of coupling loss measurements for four different embodiments of a single slot in a coaxial cable shield. The slot length and inclination with respect to the cable axis were varied.

According to the results, the strongest electric field polarization was the one longitudinal to the cable axis. This can be explained by the fact that the slot was oriented normal to the cable axis, thus cutting the longitudinal current flow, breaking the longitudinal current lines and creating the potential difference between the opposite edges of the narrower slot dimension.

Inclining the slot with respect to the cable axis did not yield any major changes for the dominant longitudinal polarization, as long as the length of the slot (measured in the cross-section projection of the slot) remained unchanged. On the other hand, the other two orthogonal polarizations gained several dB from the slot inclination, which could be important for communication between the cable and an arbitrarily polarized antenna.

The most dramatic effect occurred as the consequence of extending the length of the slot by a factor of 2, from 20% to 40% of the shield circumference. This yielded a 20 dB increase of the radiated fields, resulting with 20 dB lower coupling loss. Hence the slot length plays a major factor in designing the slot.

## REFERENCES

[1] C. A. Balanis: *Antenna theory, Analysis and Design*, John Wiley & Sons, New Jork, NY, USA, 3rd edition, 2005.

[2] Y. Li, J. Wang, Z. Zhang, and M. Chen: *Empirical Formula for the Electric Field Calculation in Rectangular Slots on Leaky Coaxial Cable*, IEEE Transactions on Antennas and Propagation, vol. 60, no. 12, pp. 5825-5833, 2012.

[3] J. F. Kiang: *Radiation Properties of Circumferential Slots on a Coaxial Cable*, IEEE Transactions on Microwave Theory and Techniques, vol. 45, no. 1, pp. 102-107, 1997.

[4] J. H. Wang and S. S. Jian: *Analysis of the Field Distribution Stimulated on the Slots of the Leaky Coaxial Cables*, in Proceedings of Antennas and Propagation Society International Symposium, vol. 3, pp. 2095-2098, July 1997.

[5] J. H. Wang and K. K. Mei: *Theory and Analysis of Leaky Coaxial Cables With Periodic Slots*, IEEE Transactions on Antennas and Propagation, vol. 49, no. 12, pp. 1723-1732, 2001

[6] J. Wei, C. Ji, and Y. Yang: *An ununiform periodic slotted leaky coaxial cable used in the specific wireless communication system of subway*, in Proceedings of 10th International Symposium on Antennas, Propagation & EM Theory, (ISAPE), pp. 1073-1076, October 2012.

[7] J. Guo and X. Liu: *Research on the Influence of Tunnel Wall on Radiation Field Caused by the Leaky Antenna*, in Proceedings of International Conference on Communications and Mobile Computing, CMC '09, vol. 1, pp. 9-13, January 2009.

[8] M. Nakamura, H. Takagi, K. Einaga, T. Nishikawa, N. Moriyama, and K. Wasaki: *Evaluation of a Dual-band Long Leaky Coaxial Cable in the 2.4 and 5 GHz Frequency Bands for Wireless Network Access*, in Proceedings of IEEE Radio and Wireless Symposium, (RWS '09), pp. 510-513, January 2009.

[9] H. Cao and Y. P. Zhang: *Radio Propagation along a Radiated Mode Leaky Coaxial Cable in Tunnels*, in Proceedings of Asia Pacific Microwave Conference, vol. 2, pp. 270-272, November 1999.

[10] J. R. Wait and D. A. Hill: *Propagation Along a Braided Coaxial Cable in a Circular Tunnel*, IEEE Transactions on Microwave Theory and Techniques, vol. MTT-23, no. 5, pp. 401-405, 1975.

[11] J. R. Wait: *Electromagnetic Field Analysis for a Coaxial Cable with Periodic Slots*, IEEE Transactions on Electromagnetic Compatibility, vol. EMC-19, no. 1, pp. 7-13, 1977.

[12] P. P. Delogne and A. A. Laloux: *Theory of the Slotted Coaxial Cable*, IEEE Transactions on Microwave Theory and Techniques, vol. MTT-28, no. 10, pp. 1102-1107, 1980.

[13] D. H. Kim and H. J. Eom: *Radiation of a Leaky Coaxial Cable with Narrow Transverse Slots*, IEEE Transactions on Antennas and Propagation, vol. 55, no. 1, pp. 107-110, 2007.

[14] T. Baba, T. Nagao, N. Kurauchi, and T. Nakahara: *Leaky Coaxial Cable with Slot Array*, in Proceedings of Antennas and Propagation Society International Symposium, vol. 6, pp. 253-258, September 1968.

[15] S. C. Dass and J. C. Beal: *Measurements on Coupled Leaky Coaxial Cables*, in Proceedings of Antennas and Propagation Society International Symposium, vol. 13, pp. 345-348, June 1975.

[16] S. T. Kim, G. H. Yun, and H. K. Park: *Numerical Analysis of the Propagation Characteristics of Multiangle Multislot Coaxial Cable Using Moment Method*, IEEE Transactions on Microwave Theory and Techniques, vol. 46, no. 3, pp. 269-279, 1998.

[17] C. W. Lee and H. Son: *Radiation Characteristics of Dielectric-Coated Coaxial Waveguide Periodic Slot with Finite and Zero Thickness*, IEEE Transactions on Antennas and Propagation, vol. 47, no. 1, pp. 16-25, 1999.

[18] J. H. Wang and S. S. Jian: *Radiation from Slots on the Leaky Coaxial Cables*, in Proceedings on IEEE Antennas and Propagation Society International Symposium, vol. 4, pp. 573-276, 2001.

[19] L. Shu, J. Wang, H. Shi, and Z. Li: *Research on the Radiation Characteristics of the Leaky Coaxial Cables*, in 6th International Symposium on Antennas, Propagation and EM Theory, pp. 242-245, October 2003.

[20] Y. Li and J. Wang: *Polarization Property of Leaky Coaxial Cable With Overlapped Triangle Slots*, IEEE Antennas and Wireless Propagation Letters, vol. 9, pp. 1049-1052, 2010.

[21] International Standard IEC 61196-4: Coaxial Communication Cables, 2nd Edition, 2004.

**Antonio Šarolić** received the Diploma Engineer, MS and PhD degrees in Electrical Engineering in 1995, 2000 and 2004 from the University of Zagreb, Croatia. He was employed at the same university from 1995 to 2005, at the Faculty of Electrical Engineering and Computing (FER), Dept. of Radiocommunications. In 2006 he joined the University of Split, FESB, Department of Electronics and is now Associate Professor in Electrical Engineering. His areas of interest are electromagnetic measurements, bioeffects of EM fields, electromagnetic compatibility (EMC) and radiocommunications.

**Zlatko Živković** received the Diploma Engineer and PhD degrees in Electrical Engineering in 2007 and 2014 from the Faculty of Electrical Engineering, Mechanical Engineering and Naval Architecture, University of Split, Croatia.
He is currently a postdoc assistant at the University of Split, Faculty of Electrical Engineering, Mechanical Engineering and Naval Architecture (FESB), Department of Electronics. His research interests are: electromagnetic measurements, bioeffects of EM fields, electromagnetic compatibility (EMC) and radiocommunications.

**Niko Ištuk** received the M.Sc degree in Communication and Information Technology in 2013 from University of Split, Faculty of Electrical Engineering, Mechanical Engineering and Naval Architecture, Split, Croatia. He is an EMC Engineer within the STRIPmed project team (Strengthening the capacity of University of Split for research, development and innovation in medical neuroelectronics) at the Speech and Hearing Research Lab, School of Medicine, University of Split, Split (Croatia).

**Damir Senić** received the M.Sc. degree in 2008 and Ph.D. degree in 2014, both from University of Split, Faculty of Electrical Engineering, Mechanical Engineering and Naval Architecture, Split, Croatia. He is currently with University of Colorado Boulder working at National Institute of Standards and Technology, Communications Technology Laboratory in Boulder as a Postdoctoral Research Associate through Professional Research Experience Program. His research interests include millimeter wave radiocommunications, electromagnetic measurements, electromagnetic compatibility (EMC) and bioeffects of EM fields. Dr. Senic received Richard E. Merwin Award of IEEE Computer Society for exemplary involvement in IEEE activities and excellent academic achievement in 2013.